Electronic Supplementary Material (ESI) for Catalysis Science & Technology.
This journal is © The Royal Society of Chemistry 2019

Electronic Supporting Information

Thermal stability and propane combustion activity of $Rh_xCe_{1-x}O_{2-y}$ nanoparticles deposited on functionalized alumina

Karolina A. Ledwa,[1*] Leszek Kępiński,[1] Mirosława Pawlyta[2]

[1]Polish Academy of Sciences, Institute of Low Temperatures and Structure Research, ul. Okólna 2, 50-422 Wrocław, Poland

[2]Silesian University of Technology, Institute of Engineering Materials and Biomaterials, ul. Konarskiego 18A, 44-100 Gliwice, Poland

***Corresponding author:**

Karolina Ledwa

K.Ledwa@intibs.pl

Tel.: (+48) 71 395 41 53

Fax**:** (+48) 71 344 10 29

Materials synthesis and treatment

Materials

Aeroxide Alu-C (Evonik-Degussa, S_{BET} = 102 m^2/g) was used as a catalyst support. Decanoic acid (98%), tetramethylammonium hydroxide (25% wt. in water) and cerium (III) nitrate hexahydrate (99.5%) were obtained from Sigma Aldrich. Cyclohexane (99%), 1-pentanol (98.5%), n-hexane (95%), ethanol (96%), and Triton X-100 were obtained from POCH. Rhodium nitrate solution (5% wt. of rhodium ions in nitric acid) was obtained from Mennica Metale Szlachetne.

Support functionalization

0.125 g of decanoic acid was dissolved in 40 cm^3 of n-hexadecane. Then Alu-C (2.5 g) was added to the solution and the mixture was stirred at room temperature for 30 min. The obtained functionalized support was then washed with hexane and ethanol and dried in the air at 60°C for 20h.

$Rh_xCe_{1-x}O_{2-y}$ nanoparticle's synthesis

To prepare the microemulsion, 85 cm^3 of cyclohexane, 13.6 cm^3 of triton X-100 and 12.2 cm^3 of 1-pentanol were mixed and intensively stirred by few minutes. Then 0.5 cm^3 of oleic acid was also added to stabilize the dispersion. Cerium nitrate hexahydrate and rhodium nitrate (5% wt. of rhodium ions in nitric acid), in appropriate molar ratio to obtain the expected mole fraction (x) of the dopant in the mixed oxide (x = 0, 0.025, 0.05, 0.075, 0.10, 0.125, 0.15), were dissolved in 6.6 cm^3 of water. Then, this solution was poured into the previously prepared organic mixture, and intensively stirred until a transparent emulsion was obtained. In the next step, 6.6 cm^3 of tetramethylammonium hydroxide (25% wt. solution in water) was slowly dropped do the mixture, and all was stirred on the magnetic stirrer for 30 min.

Sample treatment

Thermal stability of the catalysts was investigated by heating the as-prepared samples in the tube furnace at different temperatures in the oxidizing (air) or reducing (H_2, 99.95% purified additionally in the oxygen and moisture trap) gas flow for 1h or 3h. The heating rate was 5°C/min, and the pressure was 1 bar. After the H_2 treatments, the cooled samples were additionally flushed for 1h at 1 bar in the pure Ar (99.999%) to avoid the rapid oxidation in the air.

Characterization

TEM - Specimen preparation

A small amount of a powder sample was ground in a mortar and then dispersed in methanol. Next, a droplet of the suspension was put on a microscope copper grid covered with carbon. Samples were then dried and purified in a plasma cleaner. The samples subjected to a reduction in a hydrogen atmosphere, because of their high susceptibility to the oxidation processes, were prepared by putting a small amount of dry powder on the microscopic grid.

XPS

Before the measurement, the sample was heated additionally in O2 at 500°C for 30 min. at 1 bar pressure in the preparation chamber of the XPS apparatus to clean the surface. The sample was then transferred (without exposure to air) into a main chamber, where the spectra were acquired under high vacuum (2·10-10 mbar) at room temperature. A monochromatized Al Kα X-ray source (1486.6 eV, 300 W) and a hemispherical analyzer (SCIENTA EW 3000) working with the pass energy 200 eV were used.

Results

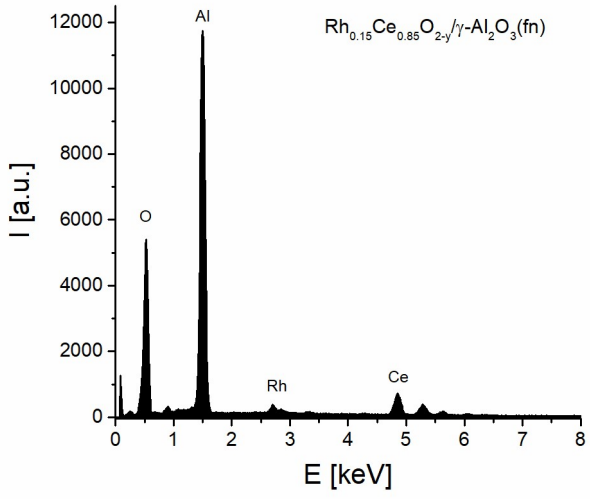

Figure S1: Example of the EDS spectrum obtained for as-prepared $Rh_{0.15}Ce_{0.85}O_{2-y}$/ γ-Al_2O_3(fn) with main peaks assigned.

Table S1. The nominal concentrations of the samples' components express as the oxides' weight percents.

Sample	x_{Rh}	Weight % of the oxide		
		Rh_2O_3	CeO_2	γ-Al_2O_3
CeO_2/γ-Al_2O_3	-	-	27.3	72.7
CeO_2/γ-Al_2O_3(fn)				
$Rh_{0.05}Ce_{0.95}O_{2-y}$	0.05	3.7	96.3	-
$Rh_{0.05}Ce_{0.95}O_{2-y}/\gamma$-$Al_2O_3$		1.0	26.0	73.0
$Rh_{0.05}Ce_{0.95}O_{2-y}/\gamma$-$Al_2O_3$(fn)				
$Rh_{0.10}Ce_{0.90}O_{2-y}$	0.10	7.6	92.4	-
$Rh_{0.10}Ce_{0.90}O_{2-y}$ /γ-Al_2O_3		2.0	24.7	73.3
$Rh_{0.10}Ce_{0.90}O_{2-y}/\gamma$-$Al_2O_3$(fn)				
$Rh_{0.15}Ce_{0.85}O_{2-y}$	0.15	11.5	88.5	-
$Rh_{0.15}Ce_{0.85}O_{2-y}$ /γ-Al_2O_3		3.1	23.4	73.5
$Rh_{0.15}Ce_{085}O_{2-y}/\gamma$-$Al_2O_3$(fn)				

Table S2: Concentrations of the selected samples' components obtained by the ICP method:

Sample	Calculated $x_{Rh} \pm SD$	Weight % of the oxide ± MU [%]		
		Rh_2O_3	CeO_2	γ-Al_2O_3
CeO_2/γ-Al_2O_3(fn)	-	-	28.3±1.4	72.8±3.6
$Rh_{0.05}Ce_{0.95}O_{2-y}/\gamma$-$Al_2O_3$(fn)	0.05	1.1±0.06	27.1±1.4	72.8±3.6
$Rh_{0.10}Ce_{0.90}O_{2-y}/\gamma$-$Al_2O_3$(fn)	0.10	1.9±0.1	24.4±1.2	71.4±3.6
$Rh_{0.15}Ce_{0.85}O_{2-y}$	0.14	10.8±0.5	87.9±4.4	-
$Rh_{0.15}Ce_{0.85}O_{2-y}$ /γ-Al_2O_3	0.15	3.1±0.2	24.3±1.2	78.0±3.9
$Rh_{0.15}Ce_{085}O_{2-y}/\gamma$-$Al_2O_3$(fn)	0.14	3.0±0.2	24.3±1.2	75.7±3.8

Table S3. Concentrations of the sample components calculated for as-prepared samples from the EDS results. The standard deviation (SD) calculated for each sample was lower than the method uncertainty (MU). The results for selected samples are presented.

Sample	Calculated $x_{Rh} \pm MU$ (SD)	Weight % of the oxide ± MU [%]		
		Rh_2O_3	CeO_2	γ-Al_2O_3
CeO_2/γ-Al_2O_3	-	-	25.1±0.5	74.9±1.5
CeO_2/γ-Al_2O_3(fn)	-	-	24.2±1.0	75.8±1.5
$Rh_{0.05}Ce_{0.95}O_{2-y}$	0.049±0.010 (0.004)	3.6±0.7	96.4±1.9	-
$Rh_{0.05}Ce_{0.95}O_{2-y}/\gamma$-$Al_2O_3$	0.077±0.015 (0.003)	1.4±0.7	22.3±1.0	76.3±1.6
$Rh_{0.05}Ce_{0.95}O_{2-y}/\gamma$-$Al_2O_3$(fn)	0.065±0.032 (0.005)	1.1±0.6	22.3±1.0	76.6±1.5
$Rh_{0.10}Ce_{0.90}O_{2-y}$	0.126±0.026 (0.025)	9.6±1.9	90.4±1.8	-
$Rh_{0.10}Ce_{0.90}O_{2-y}$ /γ-Al_2O_3	0.108±0.022 (0.008)	1.7±0.3	19.0±3.8	79.3±1.6
$Rh_{0.10}Ce_{0.90}O_{2-y}/\gamma$-$Al_2O_3$(fn)	0.111±0.022 (0.004)	2.1±0.4	22.8±4.6	75.1±1.5
$Rh_{0.15}Ce_{0.85}O_{2-y}$	0.149±0.030 (0.007)	11.5±2.3	88.5±1.8	-
$Rh_{0.15}Ce_{0.85}O_{2-y}$ /γ-Al_2O_3	0.157±0.030 (0.020)	2.8±0.6	20.6±0.8	76.6±1.5
$Rh_{0.15}Ce_{085}O_{2-y}/\gamma$-$Al_2O_3$(fn)	0.145±0.029 (0.007)	2.9±0.6	23.6±0.5	73.5±1.5

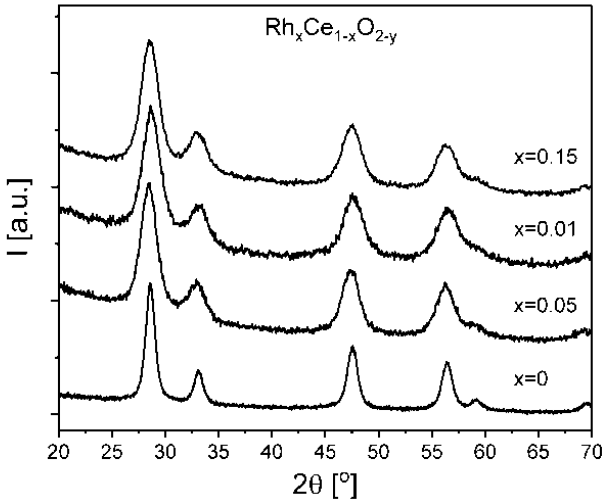

Figure S2: XRD patterns of the selected as-prepared unsupported $Rh_xCe_{1-x}O_{2-y}$ reference systems.

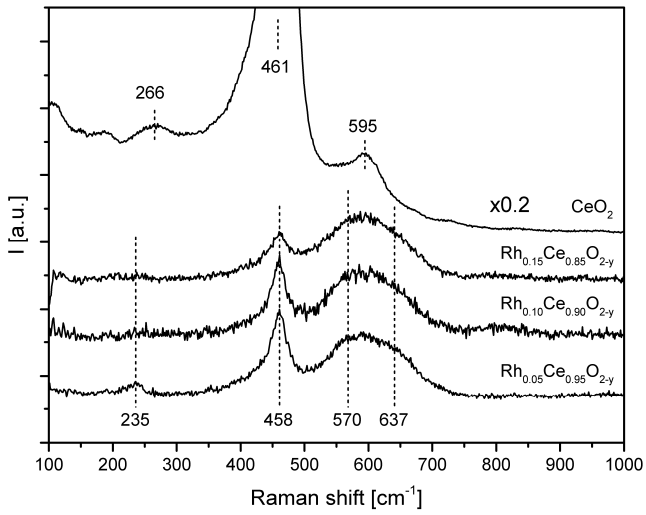

Figure S3: Raman spectra of the as-prepared unsupported $Rh_xCe_{1-x}O_{2-y}$ oxides (x = 0; 0.05; 0.10 and 0.15).

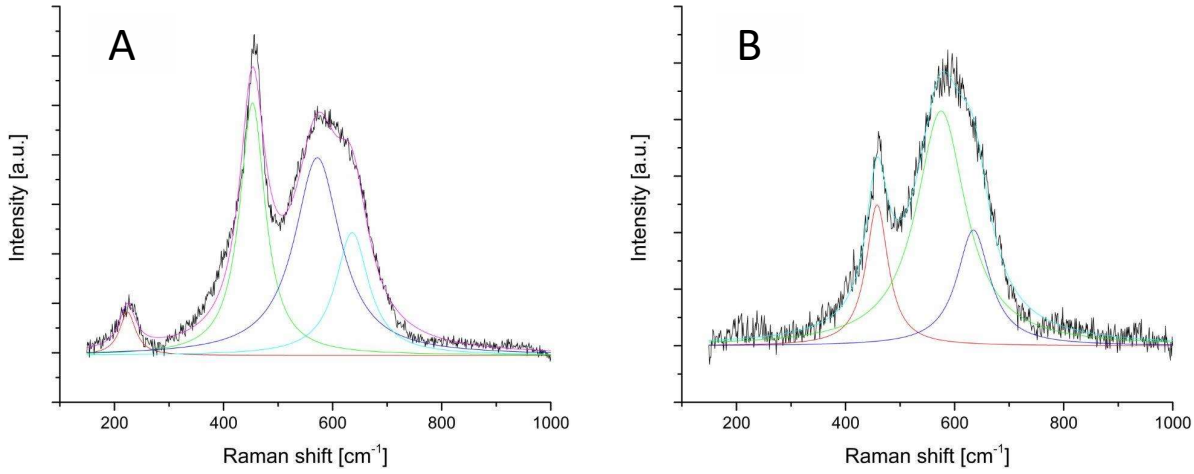

Figure S4: Deconvoluted Raman spectra of the unsupported A - $Rh_{0.05}Ce_{0.95}O_{2-y}$ and B - $Rh_{0.15}Ce_{0.85}O_{2-y}$ oxides.

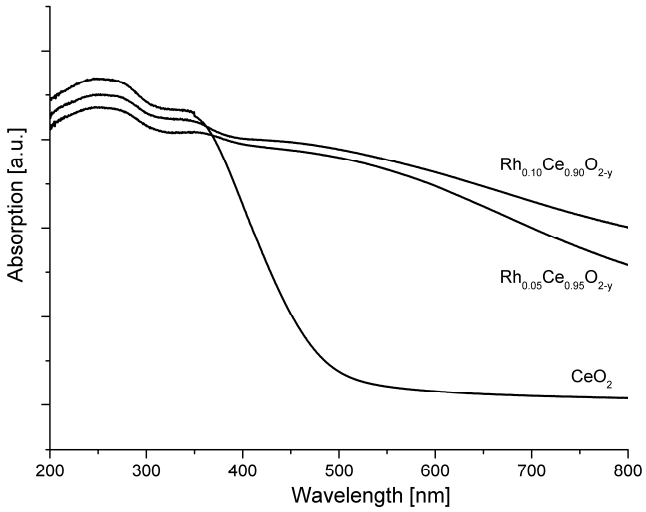

Figure S5: UV-VIS diffusion reflectance spectra of unsupported $Rh_xCe_{1-x}O_{2-y}$ oxides (x = 0; 0.05; 0.10).

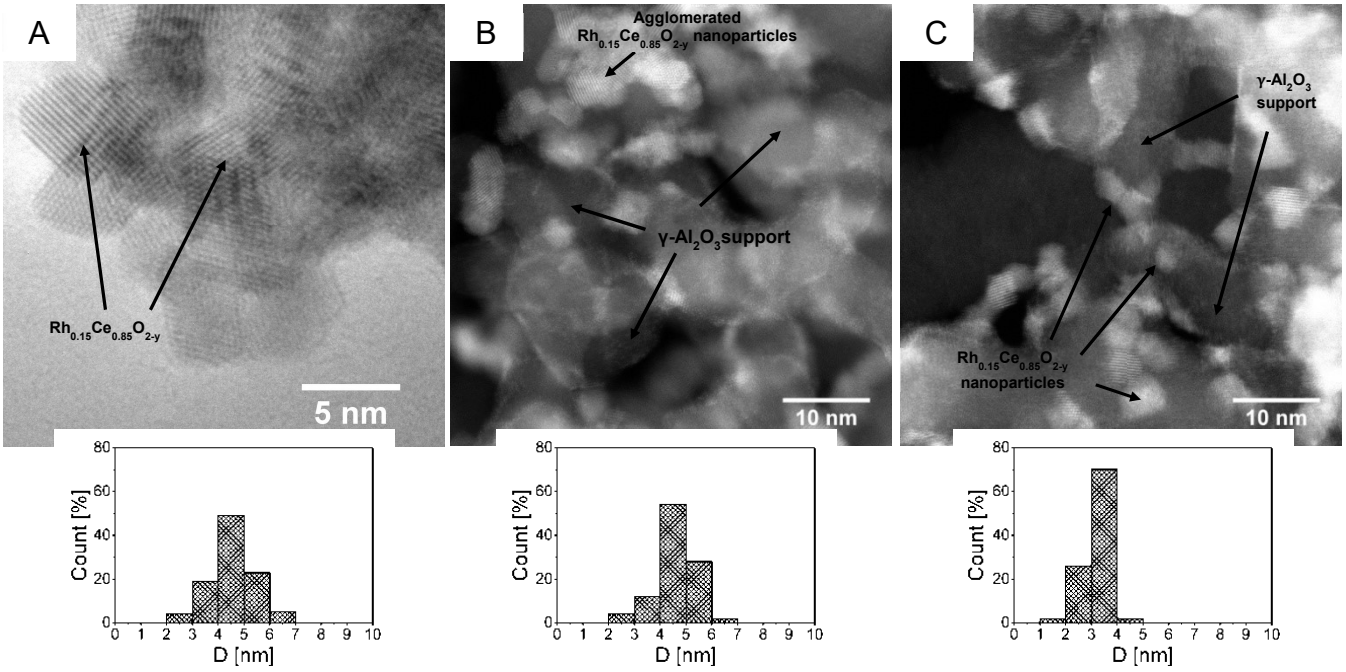

Figure S6: HRTEM (A) and STEM HAADF (B and C) images of the $Rh_{0.15}Ce_{0.85}O_{2-y}$ - unsupported (A), supported on bare (B) and decanoic acid monolayer functionalized γ-Al_2O_3, with corresponding PSDs of the $Rh_{0.15}Ce_{0.85}O_{2-y}$ nanoparticles. Results obtained for as-prepared samples.

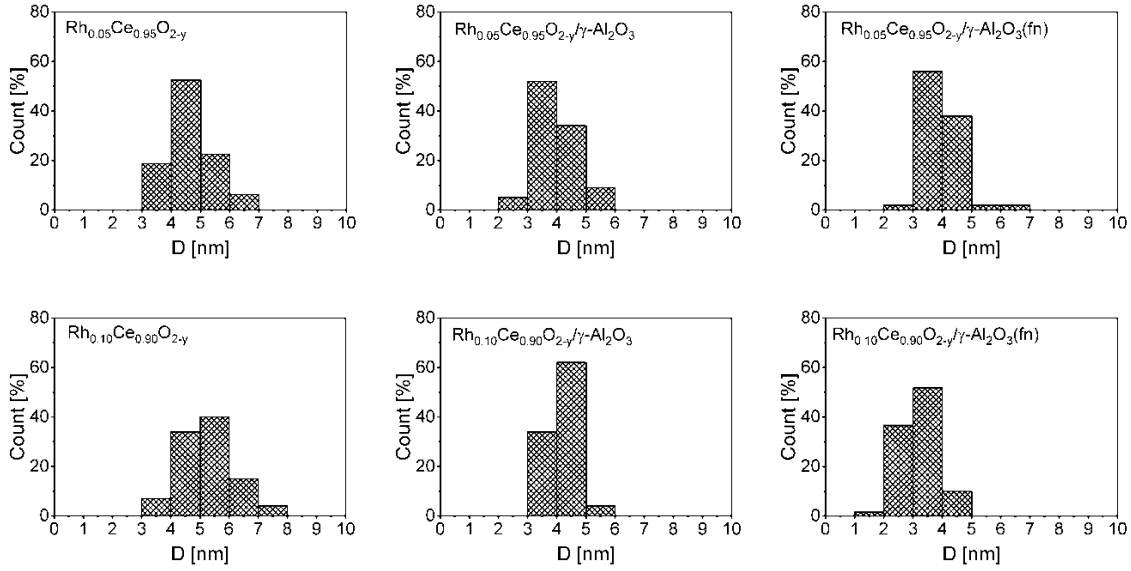

Figure S7: PSDs of the as-prepared samples containing ceria doped with Rh ions (x=0.05 and 0.010) calculated from the HRTEM images.

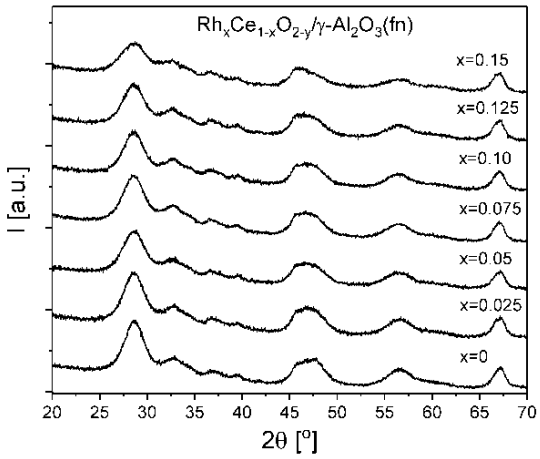

Figure S8: XRD patterns of the as-prepared $Rh_xCe_{1-x}O_{2-y}/\gamma$-$Al_2O_3$(fn) systems ($x \leq 0.15$).

Table S4: Textural properties obtained using BET method for selected as-prepared samples:

Sample	S_{BET} [m^2/g]	V_{BET} [cm^3/g]	L_{BET} [nm]
$Rh_{0.05}Ce_{0.95}O_{2-y}/\gamma$-$Al_2O_3$(fn)	107	0.63	23
$Rh_{0.10}Ce_{0.90}O_{2-y}/\gamma$-$Al_2O_3$(fn)	107	0.67	25
$Rh_{0.15}Ce_{0.85}O_{2-y}/\gamma$-$Al_2O_3$(fn)	106	0.62	24
$Rh_{0.15}Ce_{0.85}O_{2-y}/\gamma$-$Al_2O_3$	95	0.64	27
γ-Al_2O_3	102	0.98	39

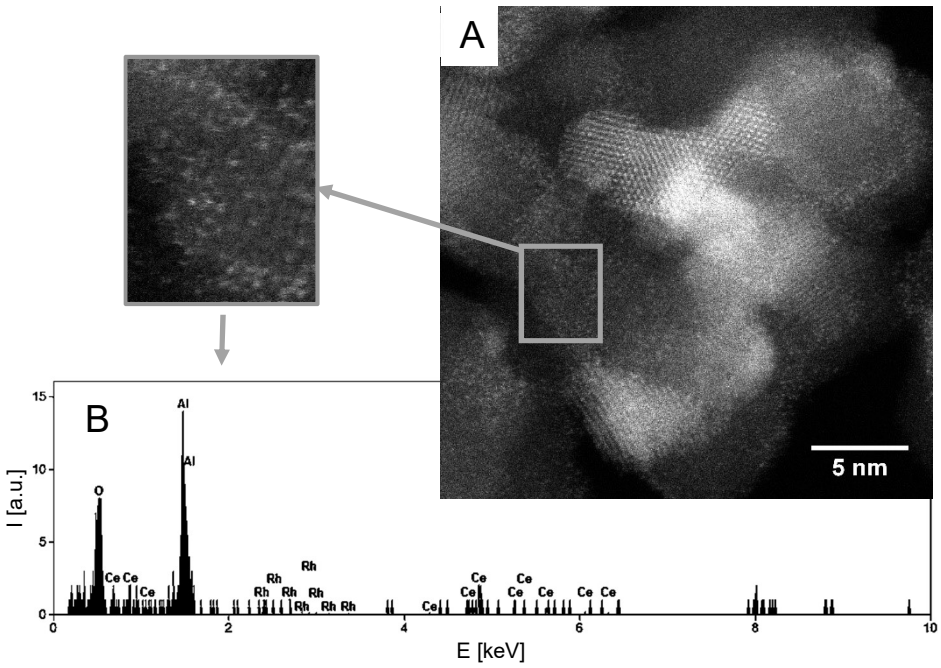

Figure S9: A - Example of STEM-HAADF image obtained for the as-prepared $Rh_{0.10}Ce_{0.90}O_{2-y}/\gamma$-$Al_2O_3$(fn) sample. Regions of atomically dispersed Ce or Rh or oxide clusters are visible. B – EDS spectrum obtained from the selected area.

Table S5: Results of the Ce3d XPS spectrum deconvolution:

Peak position	Band assignment	FWHM	Relative area [%]
882.8	v	3.35	15.6
887.9	v''	7.98	26.7
898.4	v'''	3.33	15.8
901.5	u	3.51	10.8
907.2	u''	9.13	21.4
916.9	u'''	3.37	9.7

Table S6: Results of the quantitative analysis of XPS spectrum of $Rh_{0.10}Ce_{0.90}O_{2-y}$/ γ-Al_2O_3(fn) sample:

Element	Atomic concentration [%]	Oxide	Oxide concentration [wt. %]
Rh	0.42	Rh_2O_3	2.1
Ce	2.85	CeO_2	19.6
Al	38.49	Al_2O_3	78.3
O	56.03	-	-
C	2.21	-	-

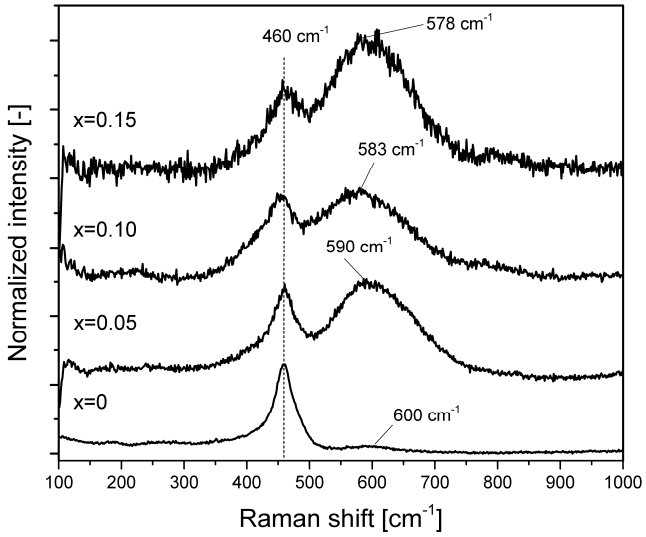

Figure S10: Raman spectra of the as-prepared $Rh_xCe_{1-x}O_{2-y}$/γ-Al_2O_3(fn) with different dopant concentrations ($x \leq 0.15$). Intensity of each spectrum was normalized to the same intensity of the F_{2g} band near 460 cm^{-1}.

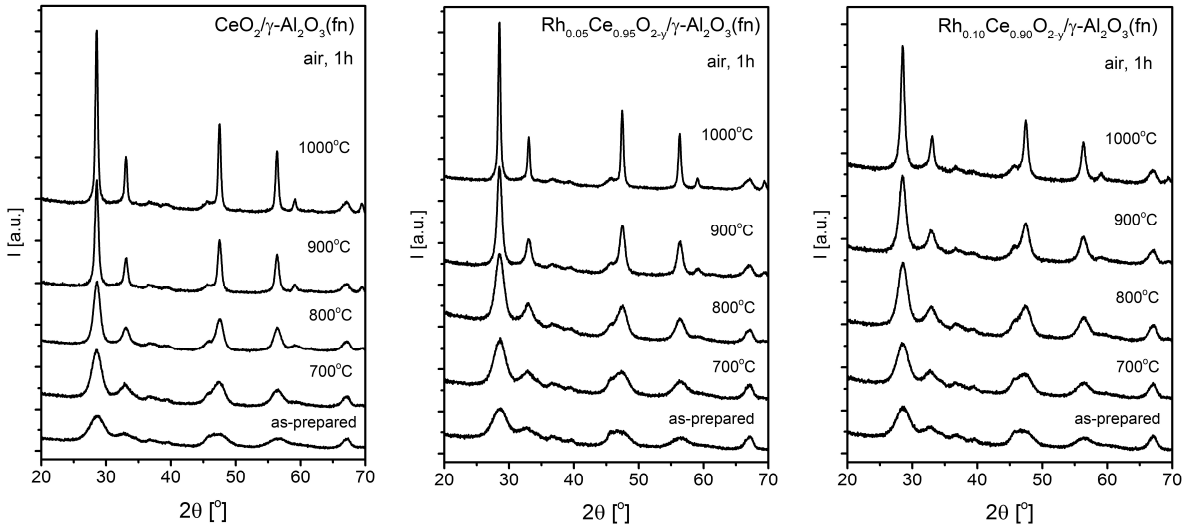

Figure S11: Results of the *ex situ* XRD measurements obtained for the samples after heating in the air for 1 h at each temperature.

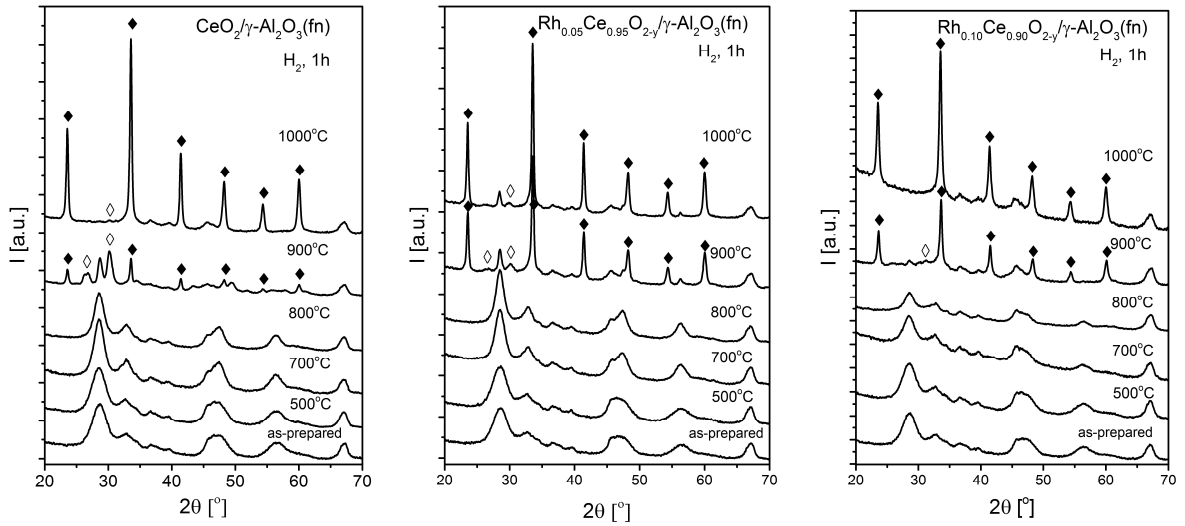

Figure S12: Results of the *ex situ* XRD measurements obtained for the samples after heating in the hydrogen for 1h at each temperature. ♦ - tetragonal $CeAlO_3$[1], ◊ - $Ce_4Al_2O_9$[2].

Table S7: Textural properties stability for bare γ-Al_2O_3 support obtained after thermal treatment in the air and in hydrogen for 3h (1 bar).

Temperature [°C]	Oxidizing atmosphere		
	S_{BET} [m^2/g]	V_{BET} [cm^3/g]	L_{BET} [nm]
800	94	0.44	19
1000	88	0.46	21
	Reducing atmosphere		
800	102	0.55	21
1000	98	0.46	19

[1] PDF: 00-048-0051

[2] L. Kępinski, J. Am. Ceram. Soc. 101 (2018) 1356–1360.

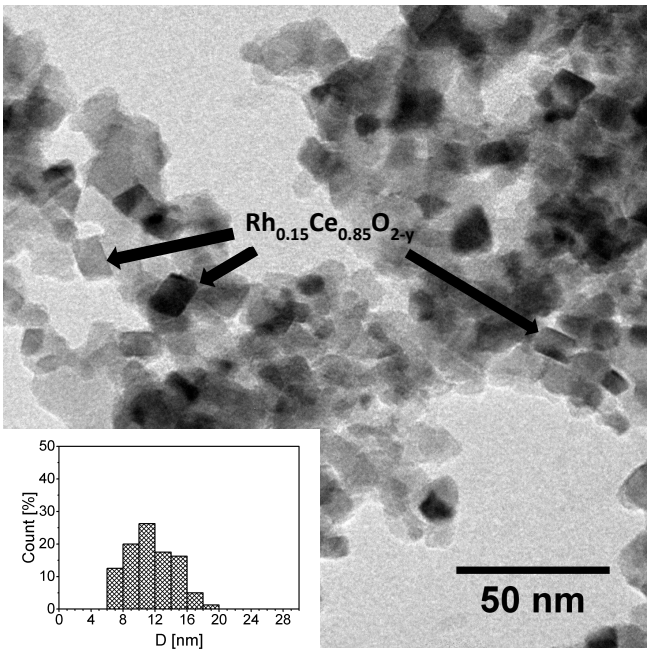

Figure S13: Representative TEM image with appropriate PSD of the $Rh_{0.15}Ce_{0.85}O_{2-y}$/ γ-Al_2O_3(fn) sample after heating in the air at 1000°C for 1h.

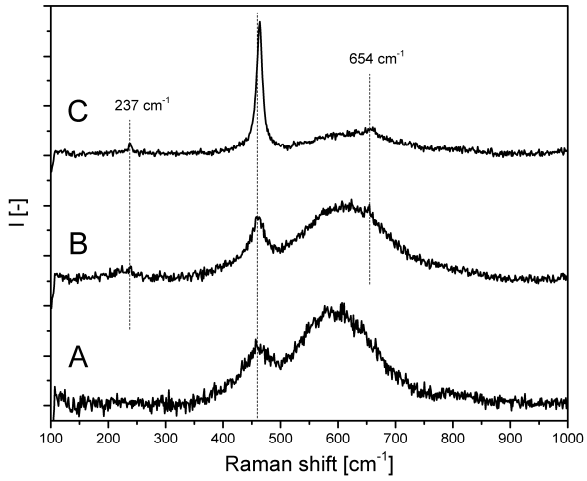

Figure S14: Raman spectra of the $Rh_{0.15}Ce_{0.85}O_{2-y}$/$\gamma$-$Al_2O_3$(fn): A – as-prepared, B – heated at 800°C and C – heated at 1000°C in the air for 1h.

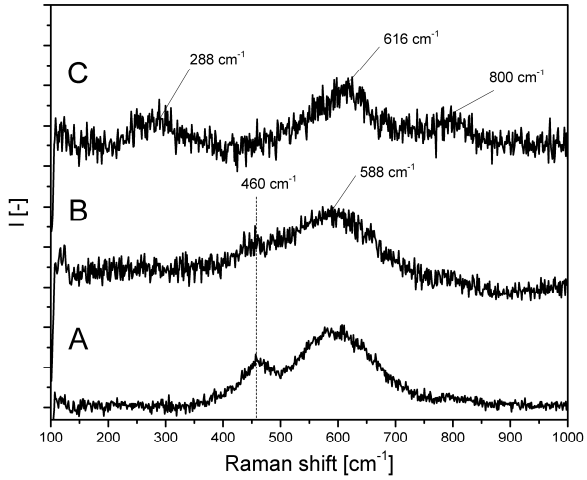

Figure S15: Raman spectra of the $Rh_{0.15}Ce_{0.85}O_{2-y}/\gamma\text{-}Al_2O_3$(fn): A – as-prepared, B – heated at 700°C and C – heated at 1000°C in the hydrogen for 1h.

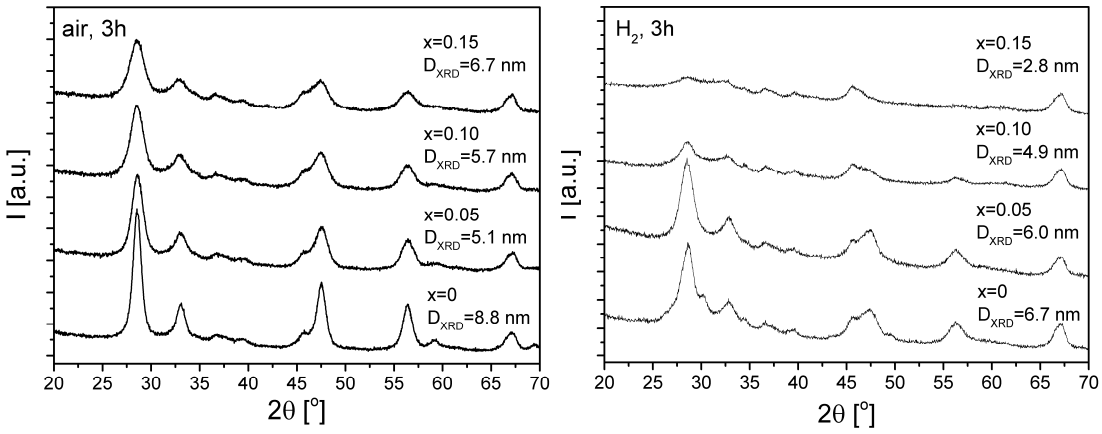

Figure S16: XRD patterns obtained *ex-situ* for $Rh_xCe_{1-x}O_{2-y}/\gamma\text{-}Al_2O_3$(fn) (x = 0; 0.05; 0.10; 0.15) samples heated in the air or in hydrogen for 3h (1 bar).

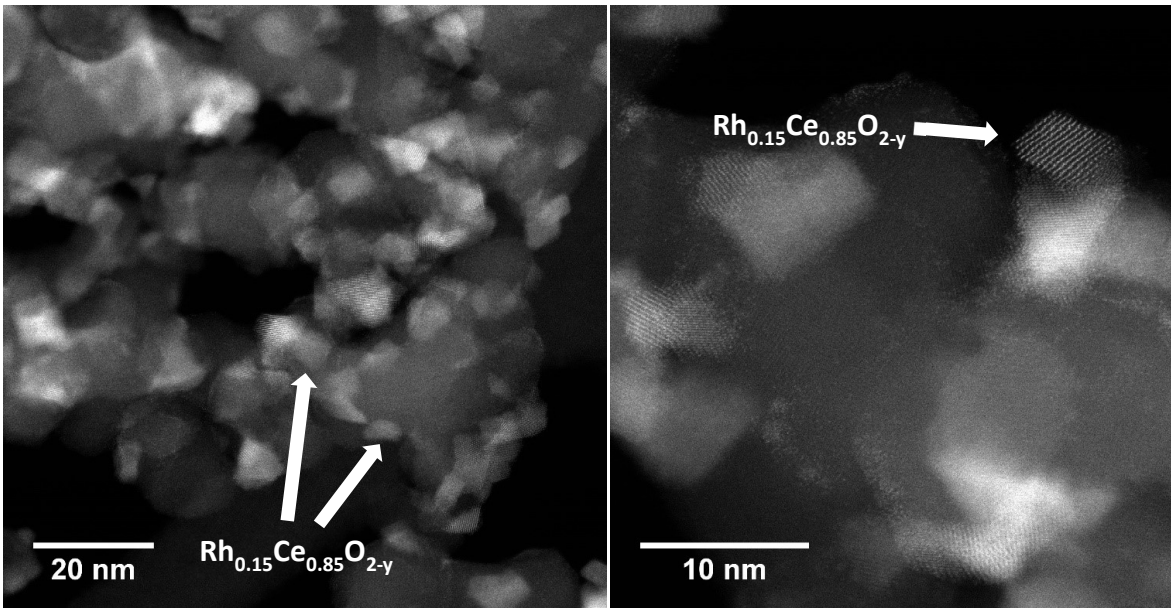

Figure S17: Examples of STEM-HAADF images obtained for $Rh_{0.15}Ce_{0.90}O_{2-y}/\gamma$-$Al_2O_3$(fn) after heating at 800°C in the air for 3h.

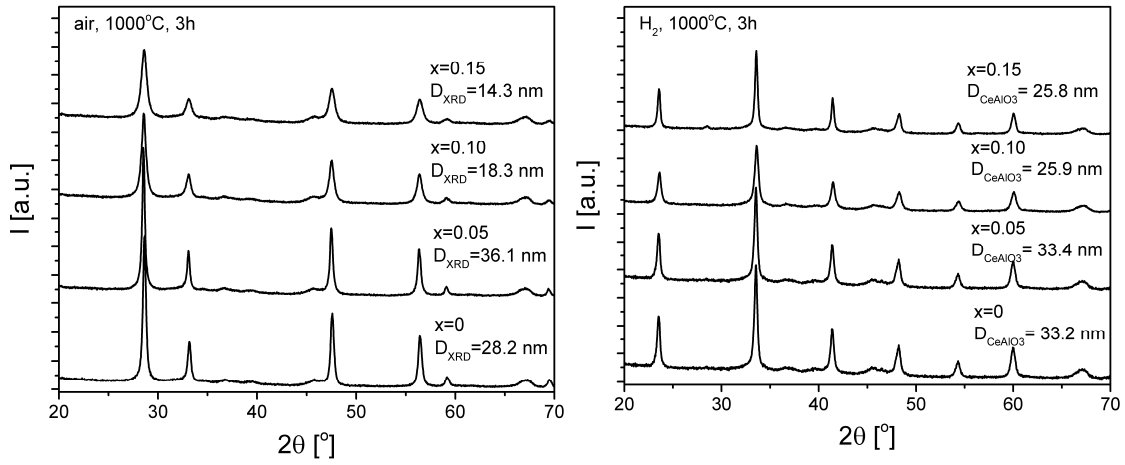

Figure S18: XRD patterns obtained for systems after heating in the air or in hydrogen at 1000°C for 3h.

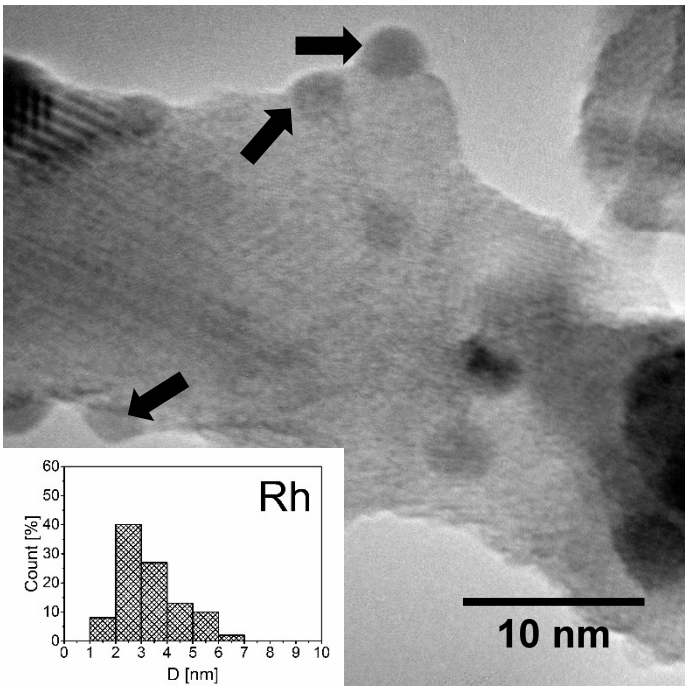

Figure S19: Example of HRTEM image of $Rh_{0.15}Ce_{0.85}O_{2-y}/\gamma\text{-}Al_2O_3$(fn) sample with PSD of metallic rhodium obtained for system after heating in the hydrogen at 900°C for 1h.

Table S8: Results of the TPR profiles analysis calculated for selected $Rh_xCe_{1-x}O_{2-y}/\gamma\text{-}Al_2O_3$(fn) ($x \leq 0.15$) samples and for the appropriate reference systems (unsupported and supported on bare alumina). Data were calculated with use of the nominal contents of metals in the samples.

Sample	≤200°C		≤500°C		≤850°C		≤1000°C	
	%Ce^{3+}	mmol H_2/g	%Ce^{3+}	mmol H_2/g	%Ce^{3+}	mmol H_2/g	%Ce^{3+}	mmol H_2/g
CeO_2[a]	0.6	0.03	6.8	0.40	23.1	1.31	28.8	1.64
$Rh_{0.05}Ce_{0.95}O_{2-y}$	8.8	0.93/0.44[b]	10.5	1.03	20.7	1.60	25.4	1.86
$Rh_{0.10}Ce_{0.90}O_{2-y}$	12.8	1.69/0.89[b]	13.9	1.71	22.4	2.26	27.5	2.56
$Rh_{0.15}Ce_{0.85}O_{2-y}$	11.4	1.86/1.28[b]	13.4	1.96	26.1	2.61	32.6	2.94
$CeO_2/\gamma\text{-}Al_2O_3$[a]	1.1	0.07	17.6	1.02	40.4	2.26	52.0	2.92
$Rh_{0.05}Ce_{0.95}O_{2-y}/\gamma\text{-}Al_2O_3$	17.5	1.42(0.44)[b]	26.3	1.91	40.6	2.71	52.4	3.37
$Rh_{0.10}Ce_{0.90}O_{2-y}/\gamma\text{-}Al_2O_3$	13.0	1.60/0.89[b]	20.7	2.04	30.9	2.56	39.6	3.03
$Rh_{0.15}Ce_{0.85}O_{2-y}/\gamma\text{-}Al_2O_3$	16.1	2.18/1.36[b]	24.3	2.60	37.0	3.25	45.9	3.71
$CeO_2/\gamma\text{-}Al_2O_3$(fn)[a]	0.8	0.05	18.9	1.10	42.8	2.49	60.4	3.51
$Rh_{0.05}Ce_{0.95}O_{2-y}/\gamma\text{-}Al_2O_3$(fn)	14.1	1.23/(0.44)[b]	27.9	2.00	44.9	2.95	55.3	3.53
$Rh_{0.10}Ce_{0.90}O_{2-y}/\gamma\text{-}Al_2O_3$(fn)	22.4	1.69(0.89)[b]	33.8	2.33	52.6	3.38	60.8	3.84
$Rh_{0.15}Ce_{0.85}O_{2-y}/\gamma\text{-}Al_2O_3$(fn)	18.8	2.32/1.36[b]	31.9	2.99	52.4	4.04	56.7	4.26

[a] Data from [3]

[b] Amount of hydrogen [mmol/g of $Rh_xCe_{1-x}O_{2-y}$] required to complete reduction of Rh^{3+} ions to Rh^0 ($Rh_2O_3+3H_2 \rightarrow 2Rh^0+3H_2O$). Rh content used in these calculations was estimated by EDS method. The component concentrations are collected in the Tab. S1.

[3] K.A. Ledwa, M. Pawlyta, L. Kępiński, Appl. Catal. B Environ. 230 (2018) 135–144.

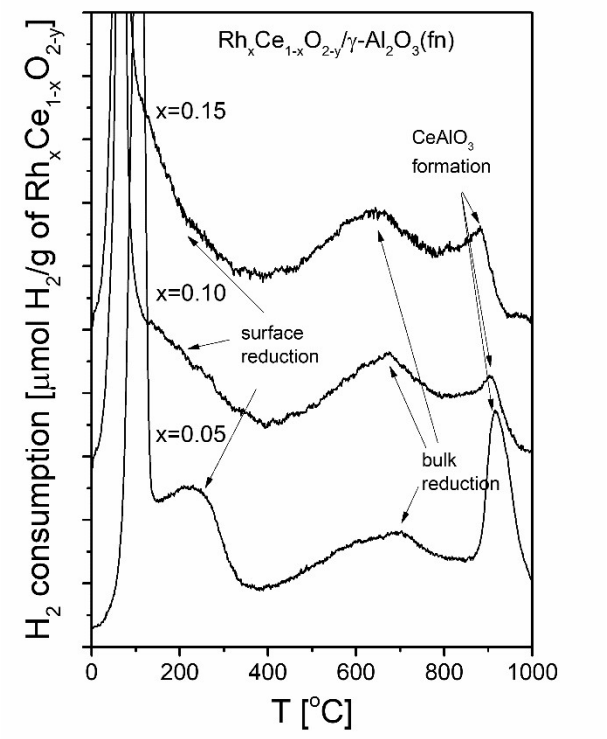

Figure S20: TPR profiles of $Rh_xCe_{1-x}O_{2-y}/\gamma$-$Al_2O_3$(fn) with different dopant concentrations - extended fragment of the profiles.

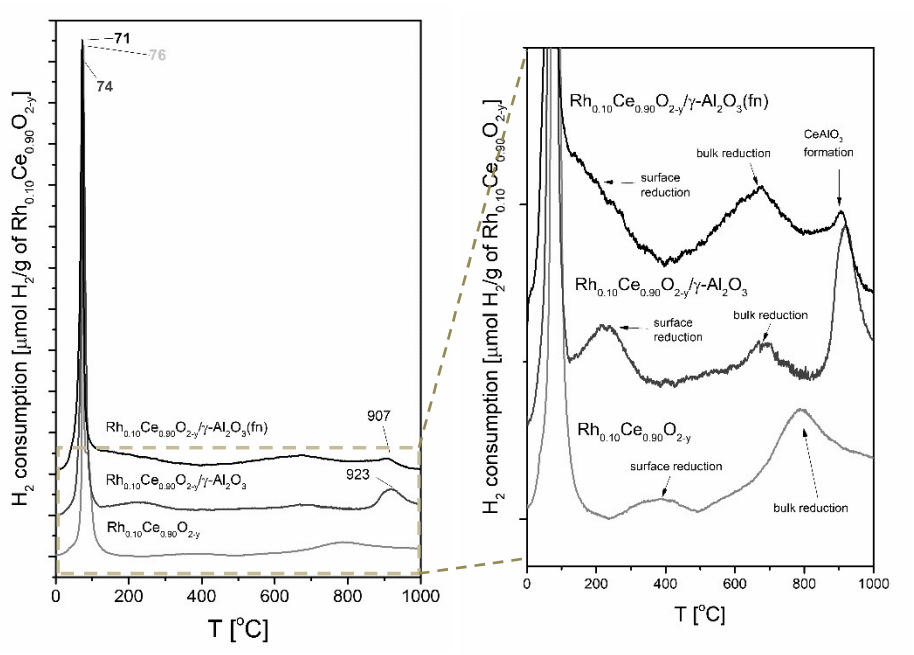

Figure S21: TPR profiles of representative $Rh_{0.10}Ce_{0.90}O_{2-y}$ unsupported, supported on bare and functionalized alumina.

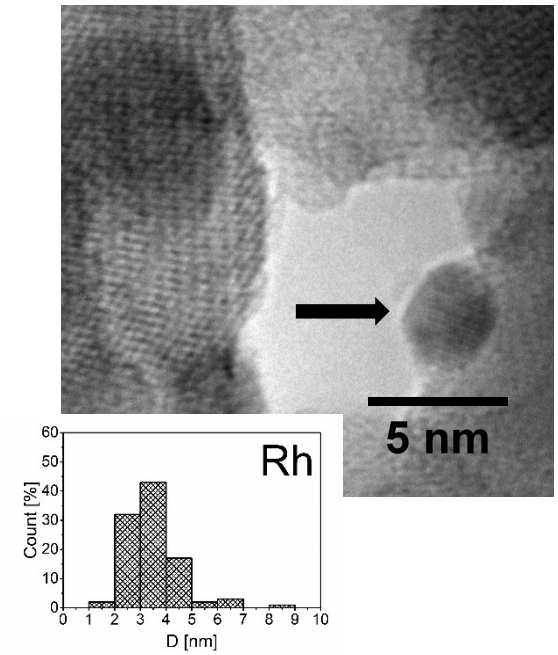

Figure S22: An example of HRTEM image obtained for $Rh_{0.15}Ce_{0.85}O_{2-y}/\gamma$-$Al_2O_3$(fn) sample with the PSD of metallic rhodium obtained for system after TPR measurement.

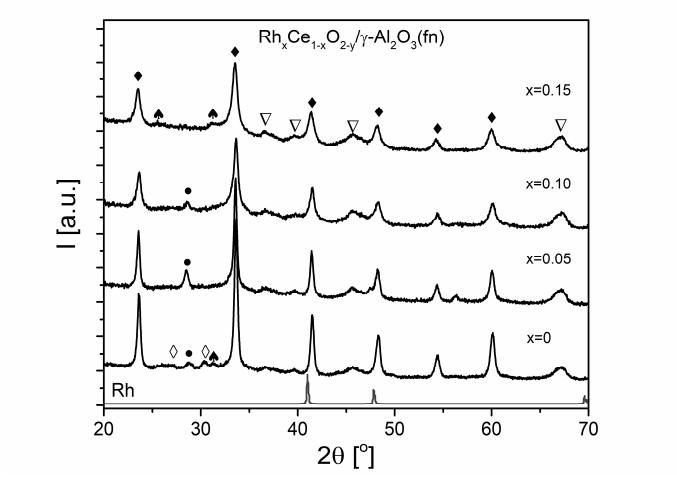

Figure S23: XRD patterns obtained for $Rh_xCe_{1-x}O_{2-y}/\gamma$-$Al_2O_3$(fn) samples after TPR measurements (up to 1000°C). XRD pattern of the reference Rh metallic phase is also presented. • - CeO_2, ∇ - γ-Al_2O_3, ♦ - tetragonal $CeAlO_3$[4], ♠ - hexagonal $CeAlO_3$[5], ◊ - $Ce_4Al_2O_9$.[6]

[4] PDF: 00-048-0051
[5] M.A. Małecka, L. Kępiński, CrystEngComm. 17 (2015) 2273–2278.
[6] L. Kępinski, J. Am. Ceram. Soc. 101 (2018) 1356–1360.

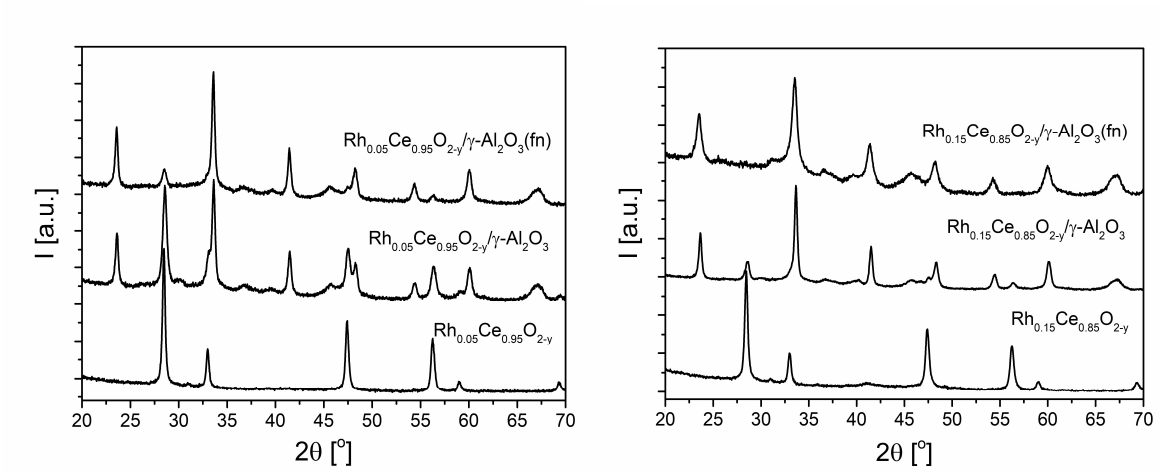

Figure S24: XRD patterns obtained for the samples after TPR measurements for $Rh_xCe_{1-x}O_{2-y}$ oxides unsupported, supported on bare and functionalized alumina (x=0.05 and 0.15).

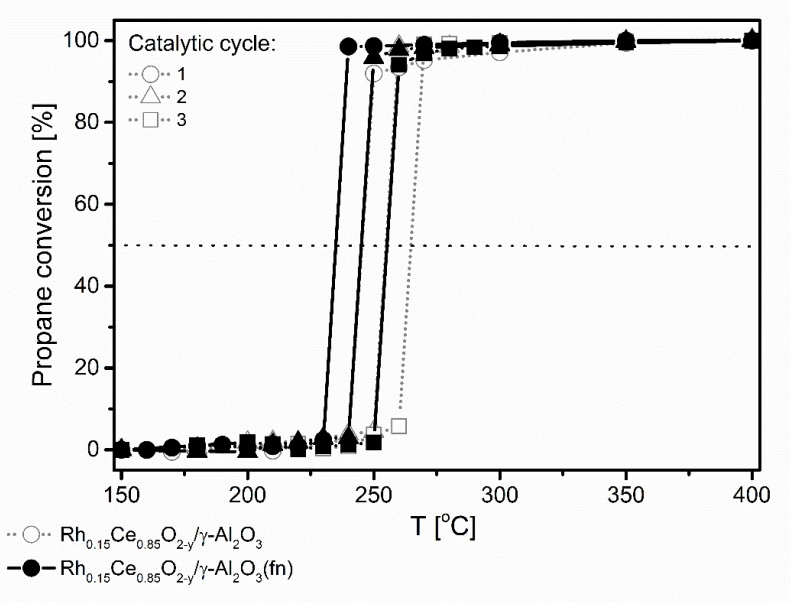

Figure S25: Propane conversion curves obtained for $Rh_{0.15}Ce_{0.85}O_{2-y}$ oxide, deposited on bare and functionalized alumina in three catalytic cycles conducted up to 400°C.

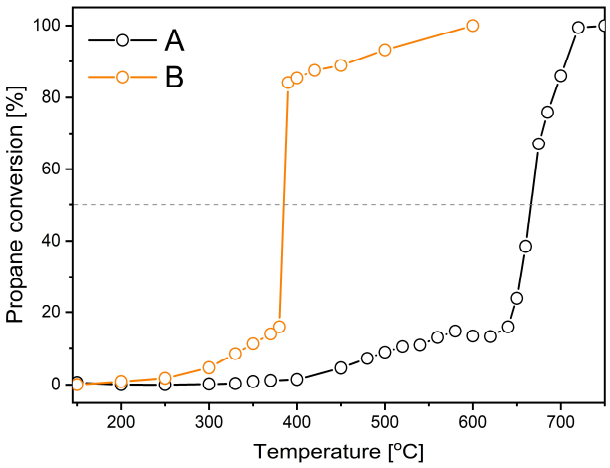

Figure S26: Propane conversion curves obtained without any catalyst – A and in the presence of the $CeO_2/\gamma\text{-}Al_2O_3$(fn) reference catalyst.

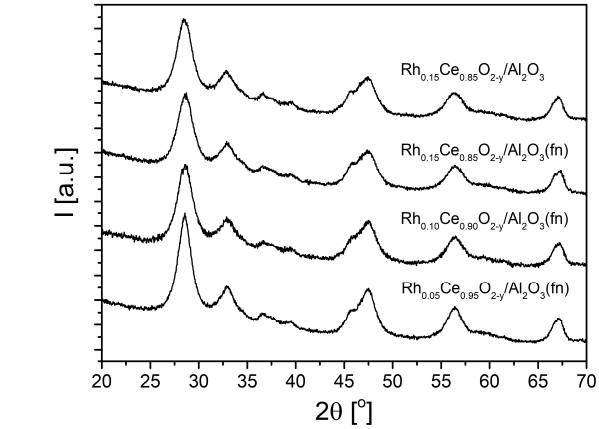

Figure S27: XRD patterns obtained for the samples after third propane oxidation cycle conducted up to 400°C.

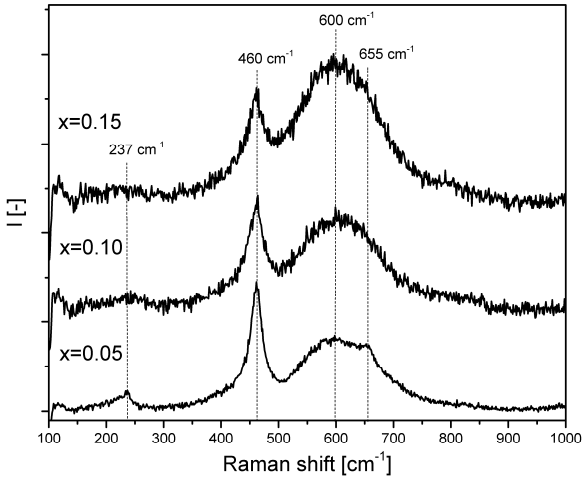

Figure S28: Raman spectra obtained for the $Rh_xCe_{1-x}O_{2-y}/\gamma\text{-}Al_2O_3$(fn) samples after third propane oxidation cycle conducted up to 400°C.